
LatentRouter: Can We Choose the Right Multimodal Model Before Seeing Its Answer?

Xueqi Cheng

Department of Computer Science
Florida State University University
xc25@fsu.edu

Yushun Dong

Department of Computer Science
Florida State University University
yushun.dong@fsu.edu

Abstract

Multimodal large language models (MLLMs) have heterogeneous strengths across OCR, chart understanding, spatial reasoning, visual question answering, cost, and latency. Effective MLLM routing therefore requires more than estimating query difficulty: a router must match the multimodal requirements of the current image-question input with the capabilities of each candidate model. We propose LATENTROUTER, a router that formulates MLLM routing as counterfactual multimodal utility prediction. Given an image-question query, LATENTROUTER extracts learned multimodal routing capsules, represents each candidate MLLM with a model capability token, and performs latent communication between these states to estimate how each model would perform if selected. A distributional outcome head predicts model-specific counterfactual quality, while a bounded capsule correction refines close decisions without allowing residual signals to dominate the prediction. The resulting utility-based policy supports performance-oriented and performance-cost routing, and handles changing candidate pools through shared per-model scoring with availability masking. Experiments on MMR-Bench and VL-RouterBench show that LATENTROUTER outperforms fixed-model, feature-level, and learned-router baselines. Additional analyses show that the gains are strongest on multimodal task groups where model choice depends on visual, layout-sensitive, or reasoning-oriented requirements, and that latent communication is the main contributor to the improvement. The code is available at: <https://github.com/LabRAI/LatentRouter>.

1 Introduction

Multimodal large language models (MLLMs) are rapidly diversifying in architecture [42, 23, 20], scale [35, 7, 3], cost [20, 28, 2], latency [20, 28, 2], and capability profile [35, 7, 22]. These models now support a broad range of vision-language tasks, including visual question answering [14, 19, 30], optical character recognition [24, 13, 41], document and chart understanding, spatial reasoning, and multimodal mathematical reasoning [25, 34, 43]. However, stronger average performance does not imply that one MLLM is uniformly best. Different models often specialize in different types of multimodal inputs: one model may be reliable on dense text and document images, another may be stronger on charts or diagrams, and another may offer a better quality-cost tradeoff for general visual question answering [37, 26, 18, 8, 9]. This heterogeneity makes MLLM routing especially important in real-world multimodal systems where many models are available, but always calling the strongest model can be unnecessarily expensive, slow, or impractical under deployment constraints.

Despite this practical need, MLLM routing remains underdeveloped compared with text-only LLM routing [26, 18]. Most existing routers for multi-LLM systems were designed for language-only inputs, where routing decisions are typically based on text-derived query features [11, 27], confidence or uncertainty estimates [44, 1], cascading policies [4, 10], or hierarchical routing structures [33, 32].

These approaches are useful when query difficulty can be inferred mainly from text, but MLLM routing is different: the best model often depends on multimodal routing signals that arise from the image, the question, and their interaction. For example, the router may need to recognize whether the input requires reading dense text, interpreting a chart, following spatial relations, comparing objects, or reasoning over a diagram before it can decide which candidate MLLM is likely to succeed. A natural workaround is to convert the image into explicit textual signals, such as captions, OCR transcripts, or predefined task labels, but these signals can be costly [15, 16], incomplete [21, 16], and insufficient when the routing-relevant information is primarily visual [29, 39, 38]. As a result, MLLM routing faces two coupled challenges: the router must preserve compact but informative multimodal routing signals from the input, and it must align these query requirements with heterogeneous model capabilities to predict which MLLM is most useful for the current query.

To address these challenges, we propose LATENTROUTER, a latent capability-matching router that formulates MLLM routing as *counterfactual multimodal utility prediction*. Instead of directly mapping a query to a fixed model ID, LATENTROUTER predicts how each candidate MLLM would perform on the current image-question input and selects the model with the highest predicted utility. To preserve compact multimodal routing signals, it extracts a small set of learned multimodal routing capsules from image and question representations. To align query requirements with model capabilities, it represents each candidate MLLM with a model capability token constructed from calibration, cost, latency, and slice-level behavior, and then performs latent communication between routing capsules and model tokens. The final model states are used for distributional counterfactual outcome prediction, while a bounded capsule correction refines close decisions without allowing noisy residual signals to dominate. The resulting utility-based rule supports performance-oriented routing, performance-cost routing, and changing model pools through shared per-model scoring with availability masking. Our main contributions are as follows:

- **A counterfactual utility formulation for MLLM routing.** We formulate MLLM routing as predicting each candidate model’s outcome on the same multimodal query. This formulation supports performance-oriented routing, performance-cost routing, and changing model pools through shared per-model utility scoring with availability masking.
- **LATENTROUTER: a latent capability-matching architecture.** We introduce a router that represents the query with learned multimodal routing capsules and represents candidate MLLMs with model capability tokens. Through latent communication, the router aligns query requirements with model capabilities and produces model-specific counterfactual utility estimates.
- **Comprehensive evaluation on MLLM routing benchmarks.** Experiments on MMR-Bench and VL-RouterBench show that LATENTROUTER outperforms fixed-model, feature-level, and learned-router baselines. Further analyses examine counterfactual outcome prediction, component ablations, task-group behavior, efficiency, and model-pool flexibility.

2 Methodology

We introduce LATENTROUTER, a latent capability-matching router for selecting among a pool of candidate MLLMs. The central idea is to treat routing as counterfactual utility prediction: before selecting a model, the router estimates how each available candidate would perform on the same image-question query. LATENTROUTER represents the query with learned multimodal routing capsules, represents each candidate MLLM with a model capability token, and aligns these two sets of latent states through latent communication. The training workflow is shown in Figure 1.

2.1 Problem Formulation

Let $x = (I, q)$ denotes a multimodal query, where I is an image and q is a natural-language question. Let $\mathcal{M} = \{m_1, \dots, m_K\}$ be the full candidate MLLM pool. For each query x , only a subset of models may be available; we denote the available index set by $\Omega(x) \subseteq \{1, \dots, K\}$. A routing trace contains the query x , the availability mask $\Omega(x)$, the observed answer quality $y_i(x)$ for each available model m_i , and model-level deployment attributes such as cost and latency. We normalize answer quality and cost to make utilities comparable across models and benchmarks.

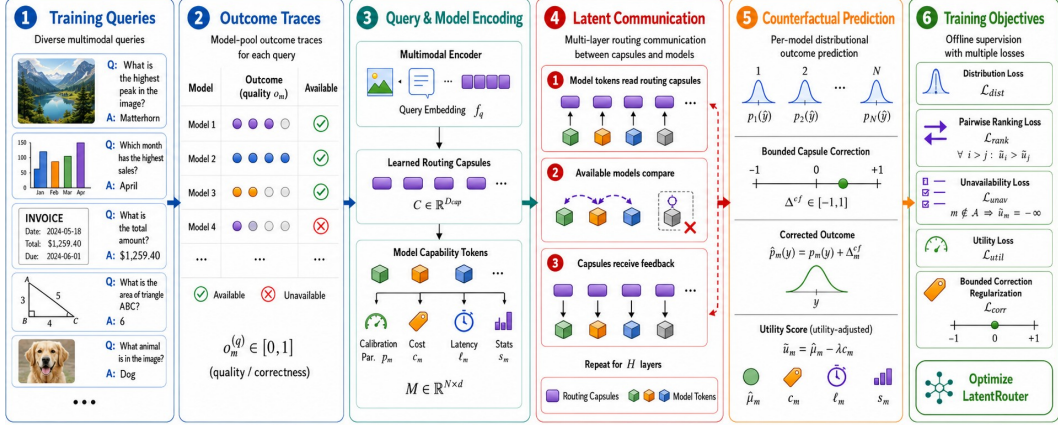


Figure 1: Training workflow of LATENTROUTER. Given an image-question query and model-pool outcome traces, the router constructs multimodal routing capsules and model capability tokens, performs latent communication, predicts per-model counterfactual outcomes, applies bounded capsule correction, and optimizes the composite training objective.

Given a cost tradeoff parameter $\lambda \geq 0$, the utility of model m_i on query x is $u_i(x) = y_i(x) - \lambda c_i$, where c_i is the normalized cost of using model m_i . When $\lambda = 0$, the objective is performance-oriented routing. When $\lambda > 0$, the objective is performance-cost routing.

A conventional router can be written as a policy $\pi_\theta(x, \mathcal{M}) \in \mathcal{M}$, which directly outputs a selected model. However, this notation hides the counterfactual structure of the problem. At routing time, the router chooses a model before observing its answer, so it must estimate how each model would perform on the same input. We therefore learn a scoring function $s_\theta(x, m_i, \mathcal{M}) \approx u_i(x)$, and select $\pi_\theta(x, \mathcal{M}) = \arg \max_{i \in \Omega(x)} s_\theta(x, m_i, \mathcal{M})$. This formulation uses the full outcome vector over the candidate pool during training. It also allows the same router to score variable model pools by masking unavailable models.

2.2 LATENTROUTER

LATENTROUTER implements $s_\theta(x, m_i, \mathcal{M})$ through latent capability matching. It consists of five components: multimodal routing capsules, model capability tokens, latent communication layers, a distributional outcome predictor, and a bounded capsule correction.

Why query-model interaction is necessary. The best MLLM depends on how the current query requirements match each candidate model’s capabilities. A router that assigns independent query and model scores cannot express query-dependent model preference reversals: the same model pair would have the same ordering for every input. However, MLLM routing often requires such reversals, e.g., one model may be better for OCR-heavy inputs while another may be better for chart or spatial reasoning. We therefore use an interaction-dependent score $s_\theta(x, m_i, \mathcal{M}) = f_\theta(R(x), a_i, A)$, where $R(x)$ denotes multimodal routing capsules, a_i is the capability token of model m_i , and A is the set of model capability tokens. Appendix B formalizes why additive scoring is insufficient.

Multimodal routing capsules. MLLM routing requires identifying which aspects of the image-question input determine model choice, such as visual text, layout, object relations, spatial cues, or image-question alignment. A single pooled query vector may blur these factors, while different candidate models may depend on different ones. LATENTROUTER therefore represents the query as a small set of learned multimodal routing capsules.

Let $V = \{v_1, \dots, v_N\}$ be image tokens and $Q = \{q_1, \dots, q_L\}$ be question tokens from a multimodal encoder. Given C learned capsule queries $\{z_k^{\text{cap}}\}_{k=1}^C$, we extract capsules by cross-attending each query to the joint image-question sequence:

$$r_k^{(0)} = \text{CrossAttn}(z_k^{\text{cap}}, [V; Q]), \quad k = 1, \dots, C.$$

The initial capsule set is $R^{(0)}(x) = \{r_1^{(0)}, \dots, r_C^{(0)}\}$. These capsules are learned latent routing states, not predefined task labels. They are trained end-to-end through the per-model outcome prediction and routing losses, so they retain information only insofar as it helps predict which candidate MLLM will perform well on the current query.

Model capability tokens. For each candidate model m_i , LATENTROUTER constructs a model capability token from model-level metadata and calibration statistics as $a_i^{(0)} = \phi([p_i; c_i; \ell_i; b_i])$. Here, p_i is the calibration profile of model m_i , c_i is normalized cost, ℓ_i is latency, and b_i contains optional slice-level or pairwise calibration statistics when available. The projection $\phi(\cdot)$ maps these features into the same hidden dimension as the routing capsules. The model-token set is $A^{(0)} = \{a_1^{(0)}, \dots, a_K^{(0)}\}$. Unavailable models are included in notation but masked in attention and scoring. This design avoids a fixed K -way model classifier: the same scoring head is shared across model tokens, and routing is performed over the currently available pool.

Latent communication. The routing capsules encode query-side multimodal requirements, while model tokens encode candidate MLLM capabilities. LATENTROUTER aligns these states through *counterfactual latent communication*: each model token reads the query capsules from its own capability perspective, model tokens compare with other available candidates, and routing capsules receive feedback from the most decision-relevant model states. This makes the communication routing-specific while keeping the intermediate process in continuous latent space.

Given routing capsules $R^{(h)} = \{r_1^{(h)}, \dots, r_C^{(h)}\}$ and model tokens $A^{(h)} = \{a_1^{(h)}, \dots, a_K^{(h)}\}$, each communication layer performs three updates. First, each model token reads the capsules through model-conditioned attention:

$$\alpha_{ik}^{(h)} = \text{softmax}_k \left(\frac{(W_q a_i^{(h)})^\top (W_k r_k^{(h)})}{\sqrt{d}} \right), \quad \hat{r}_i^{(h)} = \sum_{k=1}^C \alpha_{ik}^{(h)} W_v r_k^{(h)}.$$

The model token is then updated as $\bar{a}_i^{(h)} = \text{FFN} \left([a_i^{(h)}; \hat{r}_i^{(h)}; a_i^{(h)} \odot \hat{r}_i^{(h)}] \right)$. This produces a candidate-specific view of the query: different MLLMs can attend to different routing signals, such as visual text, layout, chart structure, or spatial cues.

Second, model tokens compare with one another through availability-masked pairwise communication. For each pair, we compute a comparison bias

$$b_{ij}^{(h)} = \psi_\theta \left([\bar{a}_i^{(h)}; \bar{a}_j^{(h)}; \bar{a}_i^{(h)} - \bar{a}_j^{(h)}; \bar{a}_i^{(h)} \odot \bar{a}_j^{(h)}] \right),$$

and inject it into masked self-attention $A^{(h+1)} = \text{SelfAttn}_{\Omega(x)} \left(\{\bar{a}_1^{(h)}, \dots, \bar{a}_K^{(h)}\}; B^{(h)} \right)$. The mask removes unavailable models, while the pairwise bias makes the update explicitly comparative. Setting $B^{(h)} = 0$ recovers standard masked self-attention.

Third, routing capsules receive decision-aware feedback from the updated model tokens. A lightweight layerwise score $s_i^{(h)}$ estimates the current utility of each available model, and feedback weights are assigned as $\omega_i^{(h)} = \text{softmax}_{i \in \Omega(x)} \left(-\frac{\max_j s_j^{(h)} - s_i^{(h)}}{\tau} \right)$. The routing capsules are updated by attending to the weighted model states $R^{(h+1)} = \text{CrossAttn} \left(R^{(h)}, \{\omega_i^{(h)} a_i^{(h+1)}\}_{i \in \Omega(x)} \right)$. This feedback emphasizes candidates near the current decision boundary, making the query representation aware of which multimodal signals distinguish the available models. After H layers, each final model token $a_i^{(H)}$ is a query-conditioned, pool-aware representation used for the next step.

Distributional counterfactual outcome prediction. For each available model, the final model token predicts a distribution over the model’s answer quality:

$$(\mu_i, \eta_i) = g_\theta(a_i^{(H)}), \quad \sigma_i = \text{softplus}(\eta_i) + \epsilon.$$

The mean μ_i estimates the expected quality of model m_i on query x , while σ_i captures predictive uncertainty. This distributional prediction is useful because routing traces provide more than the identity of the best model: they provide a full vector of observed outcomes over candidate MLLMs. Learning this vector encourages the router to model the relative strengths and weaknesses of the pool.

Bounded capsule correction. The distributional head provides a stable base estimate, but some fine-grained multimodal routing signals may still be underused. We therefore add a bounded correction from the final routing capsules:

$$\tilde{\mu}_i = \mu_i + \Delta_i^{\text{cap}}, \quad \Delta_i^{\text{cap}} = \rho \cdot \tanh\left(h_\theta([a_i^{(H)}; \text{Pool}(R^{(H)})])\right).$$

The scalar ρ limits the correction magnitude. Thus, the residual can refine close model comparisons, but cannot arbitrarily override confident base predictions. Appendix B gives more detailed proof.

Routing policy. The final routing score is the corrected predicted quality minus the cost penalty:

$$s_i(x) = \tilde{\mu}_i(x) - \lambda c_i.$$

The selected model is $\pi_\theta(x, \mathcal{M}) = \arg \max_{i \in \Omega(x)} s_i(x)$. Changing λ yields different quality-cost operating points. All unavailable models are masked before the final maximization.

2.3 Training and Deployment

Training. LATENTROUTER is trained on model-pool outcome traces. For each query, losses are computed only over available models $i \in \Omega(x)$.

The primary loss is a heteroscedastic Gaussian negative log-likelihood for normalized answer quality:

$$\mathcal{L}_{\text{dist}} = \sum_{i \in \Omega(x)} \left[\frac{(y_i - \mu_i)^2}{2\sigma_i^2} + \log \sigma_i \right].$$

This trains the distributional outcome predictor to estimate both the mean outcome and its uncertainty.

To align prediction with routing decisions, we add a pairwise ranking loss over model utilities:

$$\mathcal{L}_{\text{pair}} = \sum_{\substack{i, j \in \Omega(x) \\ u_i > u_j}} \log(1 + \exp(-(s_i - s_j))).$$

This encourages models with higher observed utility to receive higher predicted routing scores. We then use a listwise loss to match the predicted utility distribution to the observed utility distribution:

$$\mathcal{L}_{\text{list}} = \text{CE}(\text{softmax}(\mathbf{u}_\Omega/\tau), \text{softmax}(\mathbf{s}_\Omega/\tau)),$$

where \mathbf{u}_Ω and \mathbf{s}_Ω are utility and score vectors restricted to available models, and τ is a temperature. Finally, we include direct utility regression and residual regularization:

$$\mathcal{L}_{\text{util}} = \sum_{i \in \Omega(x)} (s_i - u_i)^2, \quad \mathcal{L}_{\text{res}} = \sum_{i \in \Omega(x)} (\Delta_i^{\text{cap}})^2.$$

The full training objective is $\mathcal{L} = \mathcal{L}_{\text{dist}} + \alpha \mathcal{L}_{\text{pair}} + \beta \mathcal{L}_{\text{list}} + \gamma \mathcal{L}_{\text{util}} + \eta \mathcal{L}_{\text{res}}$. The hyperparameters $\alpha, \beta, \gamma, \eta, \rho$, and τ are selected on the validation split and fixed during testing.

Deployment. At deployment time, LATENTROUTER receives a new image-question query and an available candidate model pool. It constructs routing capsules from the query, constructs model capability tokens for the available MLLMs, applies latent communication, predicts corrected outcomes $\tilde{\mu}_i$, and selects the model with the highest score $\tilde{\mu}_i - \lambda c_i$. Because the outcome predictor is shared across model tokens and unavailable models are masked, the same architecture can be applied to different model subsets without changing the classifier dimension.

3 Experimental Setup

3.1 Datasets, Models, and Metrics

We evaluate LATENTROUTER on two most recent standard MLLM routing benchmarks: MMR-Bench [26] and VL-RouterBench [18]. Both benchmarks provide image-question queries, candidate MLLM pools, per-model answer-quality annotations, and model-cost information. MMR-Bench covers OCR, general VQA, and multimodal reasoning tasks, while VL-RouterBench covers general VQA, STEM reasoning, chart/OCR, and document understanding. Following the original

benchmark settings, we evaluate 11 candidate models on MMR-Bench and 17 candidate models on VL-RouterBench; the full model lists are provided in Appendix A.

We report results under two settings. The *performance-oriented* setting evaluates whether a router selects high-quality models, while the *performance-cost* setting evaluates the quality-cost tradeoff induced by cost-aware routing. We follow the official benchmark metrics: MMR-Bench reports nAUC over the cost-quality frontier, and VL-RouterBench reports its official Rank Score.

3.2 Baselines

We compare LATENTROUTER with three groups of baselines:

- **Training-free baselines.** We include **Oracle**, **Strongest**, **Cheapest**, and **Random**. Oracle uses ground-truth outcomes and serves only as an upper bound; Strongest selects the best validation model; Cheapest selects the lowest-cost model; and Random samples uniformly from the pool.
- **Feature-level routers.** We compare with standard feature-based routers, including **KNNRouter**, **MLPMFRouter**, and **KMeansRouter**. These methods are trained on the same benchmark-provided router features and splits, and test whether conventional feature-level routing is sufficient without latent query-model interaction.
- **Learned router baselines.** We compare with the most recent MLLM router **ECVL** [31], as well as four representative text-based LLM routers, **RouteLLM** [27] **RouterDC** [5], **GraphRouter** [12] and **R2-Router** [40]. All learned baselines are adapted to the same candidate pools, splits, cost annotations, and routing features, and are implemented according to their original papers.

3.3 Implementation Details

To ensure a fair comparison, LATENTROUTER and all trainable baselines use the same benchmark-provided image features, question features, side features, model-pool metadata, cost annotations, and model-outcome traces. LATENTROUTER projects query features into a shared hidden space and summarizes them with $C = 7$ learned multimodal routing capsules. Each candidate MLLM is represented by a model capability token built from calibration profile, normalized cost, latency, and available slice-level or pairwise statistics, all computed only from the training/calibration split to avoid test-set leakage. We use $H = 2$ latent communication layers, where model tokens attend to routing capsules, interact through availability-masked self-attention, and update the capsules through feedback attention. A shared distributional outcome head predicts per-model mean and uncertainty, followed by bounded capsule correction. All trainable methods are trained on the official training split, tuned on validation, and evaluated on test over three random seeds.

4 Experiment Results

We evaluate LATENTROUTER around four questions. **RQ1:** Does LATENTROUTER improve routing performance across benchmarks and cost settings? **RQ2:** Where do the gains appear across multi-modal task types? **RQ3:** Which components are responsible for the improvement? **RQ4:** Does the router support changing candidate model pools while remaining efficient?

4.1 Main Routing Performance

For **RQ1**, Table 1 reports aggregate results on MMR-Bench and VL-RouterBench. LATENTROUTER achieves the best non-oracle result in all four settings. Compared with the strongest non-oracle baseline in each column, the improvement is statistically significant under an approximate two-sided Welch test computed from the reported mean and standard deviation over three seeds: MMR-Oriented ($p = 0.0178 < 0.05$), MMR-Cost ($p = 4.99 \times 10^{-6} < 0.001$), VL-Oriented ($p = 3.40 \times 10^{-4} < 0.001$), and VL-Cost ($p = 0.0010 < 0.01$). This pattern is important because the best competing baseline changes across benchmarks and settings: fixed-model selection is competitive in some cases, feature-level routers are strong on VL-RouterBench, and recent interaction-style routers such as GraphRouter and R2-Router narrow the gap. LATENTROUTER remains strongest across all of them, suggesting that the gain comes from a more effective query-model matching mechanism rather than from a benchmark-specific shortcut.

Table 1: Main routing performance on MMR-Bench and VL-RouterBench. MMR-Bench reports nAUC (\uparrow), and VL-RouterBench reports Rank Score (\uparrow). Best non-oracle results are in **bold**; second-best non-oracle results are underlined.

Router	MMR-Bench		VL-RouterBench	
	Oriented	Cost	Oriented	Cost
Oracle	0.918 \pm 0.000	0.899 \pm 0.000	0.932 \pm 0.000	0.932 \pm 0.000
Strongest	0.758 \pm 0.000	0.758 \pm 0.000	0.776 \pm 0.000	0.776 \pm 0.000
Cheapest	0.438 \pm 0.000	0.438 \pm 0.000	0.675 \pm 0.000	0.675 \pm 0.000
Random	0.608 \pm 0.005	0.606 \pm 0.004	0.607 \pm 0.004	0.608 \pm 0.004
KNNRouter	0.726 \pm 0.000	0.724 \pm 0.000	0.770 \pm 0.000	0.768 \pm 0.000
MLPMFRouter	0.739 \pm 0.002	0.738 \pm 0.005	0.762 \pm 0.002	0.760 \pm 0.003
KMeansRouter	0.758 \pm 0.000	<u>0.759 \pm 0.001</u>	0.781 \pm 0.004	0.782 \pm 0.004
ECVL	0.748 \pm 0.000	0.748 \pm 0.000	0.779 \pm 0.000	0.762 \pm 0.000
RouteLLM	<u>0.759 \pm 0.008</u>	0.634 \pm 0.002	0.780 \pm 0.004	0.688 \pm 0.001
RouterDC	<u>0.582 \pm 0.003</u>	0.619 \pm 0.011	0.732 \pm 0.002	0.683 \pm 0.002
GraphRouter	0.734 \pm 0.001	0.714 \pm 0.009	0.783 \pm 0.011	0.773 \pm 0.002
R2-Router	0.736 \pm 0.006	0.725 \pm 0.010	<u>0.790 \pm 0.002</u>	<u>0.785 \pm 0.004</u>
LATENTROUTER	0.792 \pm 0.001	0.786 \pm 0.001	0.815 \pm 0.001	0.812 \pm 0.003

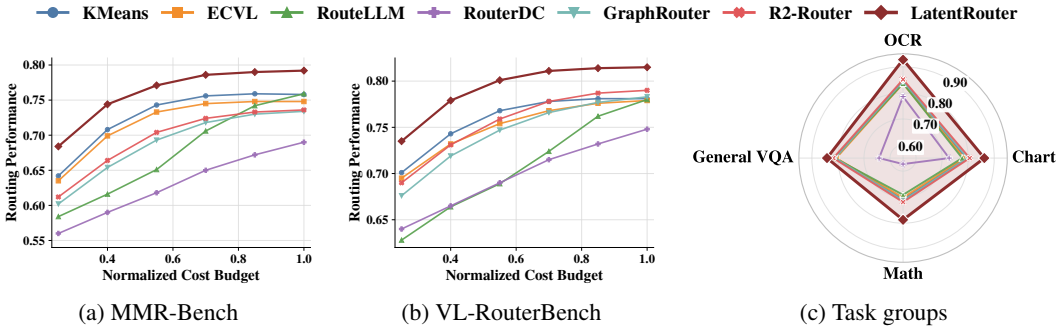


Figure 2: Cost-quality and task-level analysis. Panels (a)–(b) show cost-quality frontiers under different cost budgets; LATENTROUTER improves the frontier on both benchmarks. Panel (c) groups datasets from both benchmarks by task type; gains are largest on tasks where model choice depends strongly on visual, layout-sensitive, or reasoning-oriented query requirements.

Figure 2 further shows that the improvement is not tied to a single operating point. Figures 2a and 2b show that LATENTROUTER gives the strongest cost-quality frontier on both benchmarks, indicating that the learned utility estimate remains useful under different cost budgets. Figure 2c shows that the gains are most visible on OCR, Chart/Diagram, and Math tasks, where the best model depends on fine-grained multimodal signals such as visual text, layout, chart structure, and visual reasoning. The smaller gain on General VQA is expected because broadly strong MLLMs already perform well on many general examples, but the positive improvement still shows exploitable routing heterogeneity.

4.2 Counterfactual Outcome Prediction

For **RQ2**, Table 2 directly evaluates whether the router predicts the full counterfactual outcome vector. LATENTROUTER performs best across calibration-oriented and ranking-oriented metrics. The improvement in MSE is modest, which suggests that several methods can fit average outcome values. The more important gains appear in NDCG, Spearman correlation, and Top-3 recall, because routing depends on placing strong candidate models near the top rather than perfectly calibrating every score.

The no-communication variant isolates the role of latent communication. It uses the same query and model information, but cannot iteratively align routing capsules with model capability tokens. Its MSE remains close to the full model, while its ranking metrics are weaker. This indicates that latent

Table 2: Counterfactual outcome prediction quality. We evaluate whether each router can predict the full per-model outcome vector. Best results are in **bold**; second-best results are underlined.

Method	MSE ↓	NDCG ↑	Spearman ↑	Top-3 Recall ↑
Direct classifier	0.207 ± 0.017	0.893 ± 0.009	0.347 ± 0.077	0.269 ± 0.121
Point-score router	0.161 ± 0.012	0.913 ± 0.011	0.413 ± 0.078	0.268 ± 0.025
No latent communication	0.162 ± 0.012	0.912 ± 0.010	0.411 ± 0.079	<u>0.274 ± 0.033</u>
LATENTROUTER	0.159 ± 0.012	0.915 ± 0.009	0.425 ± 0.074	0.283 ± 0.050

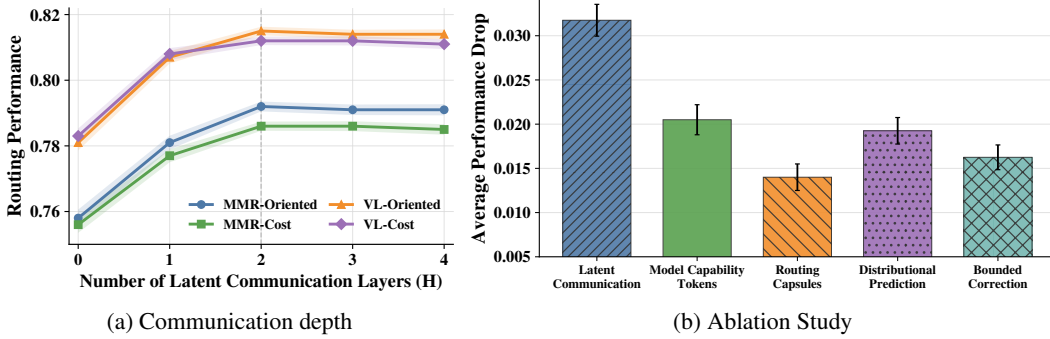


Figure 3: Mechanism analysis. (a) Performance improves quickly and saturates after $H = 2$, supporting a shallow latent communication design. (b) Ablations show latent communication is the key component, with other modules providing complementary gains.

communication mainly improves the relative ordering of candidate MLLMs, especially among top candidates where the final routing decision is made.

4.3 Mechanism Analysis

For **RQ3**, Figure 3 explains how the main components contribute to routing performance. Figure 3a shows that moving from $H = 0$ to $H = 1$ gives a clear gain, meaning that even one round of communication between routing capsules and model capability tokens is useful. Performance reaches its best or near-best value at $H = 2$ and then saturates. This is expected because each communication layer already contains a full query-model-pool update: model tokens read routing capsules, compare with other available model tokens, and send feedback to the capsules. After two rounds, the main routing-relevant alignment has largely been formed, so additional layers mostly repeat similar comparisons rather than introducing new information.

Figure 3b gives the component-level view. Removing latent communication causes the largest drop, confirming it as the central mechanism. Removing model capability tokens or routing capsules also hurts, showing that the router needs both model-side capability information and query-side multimodal routing signals. The distributional prediction head and bounded correction provide smaller but consistent gains: the former improves counterfactual outcome estimation, while the latter helps refine close model comparisons without destabilizing the base prediction. Together, these results show that LATENTROUTER’s gains come from the intended capsule-token matching process.

4.4 Model-Pool Flexibility and Efficiency

For **RQ4**, Figure 4 evaluates whether LATENTROUTER remains useful when the available model pool changes and whether the router itself is lightweight. In Figure 4a, performance drops most when the strongest model is removed, which reflects the lower ceiling of the remaining pool. Removing the cheapest model has little effect on the primary metric, while random removal and leave-one-model-out produce intermediate changes. This pattern suggests that LATENTROUTER can mask unavailable models and re-rank the remaining candidates through shared model-token scoring.

Figure 4b shows the same behavior from the oracle-regret perspective. Regret increases when useful models are removed, but remains bounded under non-degenerate pool changes, indicating that the

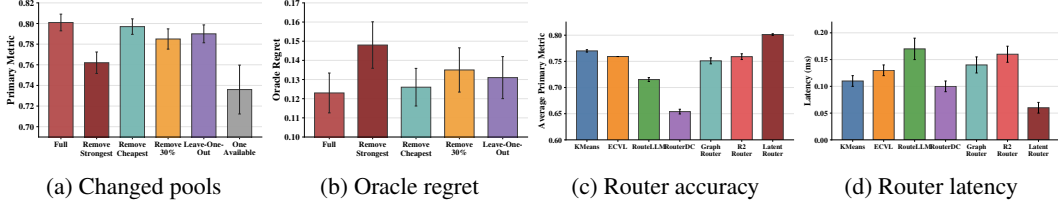


Figure 4: Model-pool flexibility and efficiency analysis. (a)–(b) LATENTROUTER handles changed candidate pools through availability masking and re-ranking. (c)–(d) It achieves the best average primary metric with the lowest router latency among learned routers.

router still makes meaningful selections over the available subset. Figures 4c and 4d summarize router-side efficiency. LATENTROUTER achieves the best average primary metric while maintaining the lowest router latency among learned methods. This shows that the capsule-token communication module improves model selection while keeping router overhead small relative to MLLM inference.

5 Related Work

Routing in Multi-LLM and MLLM Systems. Routing in text-only multi-LLM systems has been widely studied as a way to improve the quality-cost tradeoff by selecting an appropriate model for each query. Prior work uses query-level preference or difficulty signals [27, 11], confidence or uncertainty estimates [44], cascading policies [4, 10], benchmark-driven formulations [17], or hierarchical structures [33]. These methods provide useful foundations, but they are primarily designed for language-only inputs. MLLM routing introduces additional multimodal signals, such as OCR density, chart layout, visual grounding, spatial relations, and diagram-based reasoning, that may not be recoverable from the question text alone. Recent benchmarks formalize this setting: MMR-Bench studies MLLM routing under controlled model pools, task mixtures, and cost budgets [26], while VL-RouterBench shows substantial routability in vision-language model pools and a remaining gap to oracle selection [18]. Our work complements these by proposing a novel MLLM router architecture for counterfactual utility prediction.

Latent reasoning. Latent reasoning studies whether intermediate computation can be carried out in continuous hidden states instead of being fully verbalized in natural language [6, 45]. Coconut shows that language models can reuse hidden states as continuous reasoning states in later computation [15]. In multimodal reasoning, PLUME argues that verbalized chain-of-thought can create a bottleneck for rich visual information and explores latent rollouts for multimodal representations [16]; Modal-Mixed CoT studies reasoning with both text and latent visual sketches when intermediate states are not naturally expressed as text [29]; and Monet investigates latent visual reasoning through intermediate visual thoughts [36]. More broadly, prior work on vision-language models suggests that textual or pooled representations can lose compositional visual information [21]. Our work is related in motivation, but uses latent communication for a different purpose: the latent states are optimized to predict outcomes for routing, not to generate intermediate reasoning traces within a single MLLM.

6 Conclusion

We introduced LATENTROUTER, an MLLM router that formulates model selection as counterfactual multimodal utility prediction. Instead of directly classifying a query into a model ID, LATENTROUTER matches multimodal routing capsules with model capability tokens through latent communication, predicts per-model counterfactual outcomes, and selects by utility. Experiments on MMR-Bench and VL-RouterBench show consistent gains over fixed-model, feature-level, and learned-router baselines in both performance-oriented and performance-cost settings. Further analyses indicate that the gains are strongest on visually and reasoning-intensive task groups, and that latent communication is the key component. Future work includes live deployment studies, adaptive calibration for newly added MLLMs, and extensions to multi-step multimodal routing.

References

- [1] Pranjal Aggarwal, Aman Madaan, Ankit Anand, Srividya Pranavi Potharaju, Swaroop Mishra, Pei Zhou, Aditya Gupta, Dheeraj Rajagopal, Karthik Kappaganthu, Yiming Yang, Shyam Upadhyay, Manaal Faruqui, and Mausam. Automix: Automatically mixing language models. *arXiv preprint arXiv:2310.12963*, 2023.
- [2] Jyoti Aneja, Michael Harrison, Neel Joshi, Tyler LaBonte, John Langford, and Eduardo Salinas. Phi-4-reasoning-vision-15b technical report. *arXiv preprint arXiv:2603.03975*, 2026.
- [3] Shuai Bai, Keqin Chen, Xuejing Liu, Jialin Wang, Wenbin Ge, Siboz Song, Kai Dang, Peng Wang, Shijie Wang, Jun Tang, et al. Qwen2.5-vl technical report. *arXiv preprint arXiv:2502.13923*, 2025.
- [4] Lingjiao Chen, Matei Zaharia, and James Zou. Frugalgpt: How to use large language models while reducing cost and improving performance. *arXiv preprint arXiv:2305.05176*, 2023.
- [5] Shuhao Chen, Weisen Jiang, Baijiong Lin, James Kwok, and Yu Zhang. Routerdc: Query-based router by dual contrastive learning for assembling large language models. *Advances in Neural Information Processing Systems*, 37:66305–66328, 2024.
- [6] Xinghao Chen, Anhao Zhao, Heming Xia, Xuan Lu, Hanlin Wang, Yanjun Chen, Wei Zhang, Jian Wang, Wenjie Li, and Xiaoyu Shen. Reasoning beyond language: A comprehensive survey on latent chain-of-thought reasoning. *arXiv preprint arXiv:2505.16782*, 2025.
- [7] Zhe Chen, Weiyun Wang, Yue Cao, Yutong Liu, Zhangwei Gao, Erfei Cui, et al. Expanding performance boundaries of open-source multimodal models with model, data, and test-time scaling. *arXiv preprint arXiv:2412.05271*, 2024.
- [8] Xueqi Cheng, Catherine Yang, Yuying Zhao, Yu Wang, Hamid Karimi, and Tyler Derr. Bts: A comprehensive benchmark for tie strength prediction. In *Proceedings of the 31st ACM SIGKDD Conference on Knowledge Discovery and Data Mining V. 2*, pages 5345–5354, 2025.
- [9] Xueqi Cheng, Minxing Zheng, Shixiang Zhu, and Yushun Dong. Misleader: Defending against model extraction with ensembles of distilled models. *arXiv preprint arXiv:2506.02362*, 2025.
- [10] Jasper Dekoninck, Maximilian Baader, and Martin Vechev. A unified approach to routing and cascading for llms. *arXiv preprint arXiv:2410.10347*, 2024.
- [11] Dujian Ding, Ankur Mallick, Chi Wang, Robert Sim, Subhabrata Mukherjee, Victor Ruhle, Laks V. S. Lakshmanan, and Ahmed Hassan Awadallah. Hybrid llm: Cost-efficient and quality-aware query routing. *arXiv preprint arXiv:2404.14618*, 2024.
- [12] Tao Feng, Yanzhen Shen, and Jiaxuan You. Graphrouter: A graph-based router for llm selections. *arXiv preprint arXiv:2410.03834*, 2024.
- [13] Ling Fu, Biao Yang, Zhebin Kuang, Jiajun Song, Yuzhe Li, Linghao Zhu, Qidi Luo, Xinyu Wang, Hao Lu, Mingxin Huang, Zhang Li, Guozhi Tang, Bin Shan, Chunhui Lin, Qi Liu, Binghong Wu, Hao Feng, Hao Liu, Can Huang, Jingqun Tang, Wei Chen, Lianwen Jin, Yuliang Liu, and Xiang Bai. Ocrbench v2: An improved benchmark for evaluating large multimodal models on visual text localization and reasoning. *arXiv preprint arXiv:2501.00321*, 2025.
- [14] Yash Goyal, Tejas Khot, Douglas Summers-Stay, Dhruv Batra, and Devi Parikh. Making the V in VQA: Elevating the role of image understanding in visual question answering. In *Proceedings of the IEEE Conference on Computer Vision and Pattern Recognition*, pages 6904–6913, 2017.
- [15] Shibo Hao, Sainbayar Sukhbaatar, DiJia Su, Xian Li, Zhiting Hu, Jason E. Weston, and Yuandong Tian. Training large language models to reason in a continuous latent space. *arXiv preprint arXiv:2412.06769*, 2025.
- [16] Chenwei He, Xiangzhao Hao, Tianyu Yang, Yuxiang Ma, Yuheng Jia, Lingxiang Wu, Chaoyang Zhao, Haiyun Guo, and Jinqiao Wang. Plume: Latent reasoning based universal multimodal embedding. *arXiv preprint arXiv:2604.02073*, 2026.

- [17] Qitian Jason Hu, Jacob Bieker, Xiuyu Li, Nan Jiang, Benjamin Keigwin, Gaurav Ranganath, Kurt Keutzer, and Shriyash Kaustubh Upadhyay. Routerbench: A benchmark for multi-llm routing system. *arXiv preprint arXiv:2403.12031*, 2024.
- [18] Zhehao Huang, Baijiong Lin, Jingyuan Zhang, Jingying Wang, Yuhang Liu, Ning Lu, Tao Li, and Xiaolin Huang. Vl-routerbench: A benchmark for vision-language model routing, 2025.
- [19] Drew A. Hudson and Christopher D. Manning. Gqa: A new dataset for real-world visual reasoning and compositional question answering. In *Proceedings of the IEEE/CVF Conference on Computer Vision and Pattern Recognition*, pages 6700–6709, 2019.
- [20] Yizhang Jin, Jian Li, Yexin Liu, Tianjun Gu, Kai Wu, Zhengkai Jiang, Muyang He, Bo Zhao, Xin Tan, Zhenye Gan, Yabiao Wang, Chengjie Wang, and Lizhuang Ma. Efficient multimodal large language models: A survey. *arXiv preprint arXiv:2405.10739*, 2024.
- [21] Amita Kamath, Jack Hessel, and Kai-Wei Chang. Text encoders bottleneck compositionality in contrastive vision-language models. *arXiv preprint arXiv:2305.14897*, 2023.
- [22] Bo Li, Yuanhan Zhang, Pengchuan Li, Zicheng Zhang, Fanyi Pu, Ziwei Liu, et al. Llava-onevision: Easy visual task transfer. *arXiv preprint arXiv:2408.03326*, 2024.
- [23] Cheng-Xu Liang, Yaoyuan Tian, Li Ming, Tianyang Wang, Ziqian Bi, Ming Liu, et al. A comprehensive survey and guide to multimodal large language models in vision-language tasks. *arXiv preprint arXiv:2411.06284*, 2024.
- [24] Yuliang Liu, Zhang Li, Mingxin Huang, Biao Yang, Wenwen Yu, Chunyuan Li, Xucheng Yin, Cheng-Lin Liu, Lianwen Jin, and Xiang Bai. Ocrbench: On the hidden mystery of ocr in large multimodal models. *arXiv preprint arXiv:2305.07895*, 2023.
- [25] Pan Lu, Hritik Bansal, Tony Xia, Jiacheng Liu, Chunyuan Li, Hannaneh Hajishirzi, Hao Cheng, Kai-Wei Chang, Michel Galley, and Jianfeng Gao. Mathvista: Evaluating mathematical reasoning of foundation models in visual contexts. *arXiv preprint arXiv:2310.02255*, 2023.
- [26] Haoxuan Ma, Guannan Lai, and Han-Jia Ye. Mmr-bench: A comprehensive benchmark for multimodal llm routing. *arXiv preprint arXiv:2601.17814*, 2026.
- [27] Isaac Ong, Amjad Almahairi, Vincent Wu, Wei-Lin Chiang, Tianhao Wu, Joseph E. Gonzalez, M. Waleed Kadous, and Ion Stoica. Routellm: Learning to route llms with preference data. *arXiv preprint arXiv:2406.18665*, 2024.
- [28] Haoran Qiu, Anish Biswas, Zihan Zhao, Jayashree Mohan, Alind Khare, Esha Choukse, Inigo Goiri, Zeyu Zhang, Haiying Shen, Chetan Bansal, Ramachandran Ramjee, and Rodrigo Fonseca. Modserve: Modality- and stage-aware resource disaggregation for scalable multimodal model serving. *arXiv preprint arXiv:2502.00937*, 2025.
- [29] Yifei Shao, Kun Zhou, Ziming Xu, Mohammad Atif Quamar, Shibo Hao, Zhen Wang, Zhit-ing Hu, and Biwei Huang. Learning modal-mixed chain-of-thought reasoning with latent embeddings. *arXiv preprint arXiv:2602.00574*, 2026.
- [30] Amanpreet Singh, Vivek Natarajan, Meet Shah, Yu Jiang, Xinlei Chen, Devi Parikh, Marcus Rohrbach, and Dhruv Batra. Towards vqa models that can read. In *Proceedings of the IEEE/CVF Conference on Computer Vision and Pattern Recognition*, pages 8317–8326, 2019.
- [31] Xin Tang, Youfang Han, Fangfei Gou, Wei Zhao, Xin Meng, Yang Yu, Jinguo Zhang, Yuanchun Shi, Yuntao Wang, and Tengxiang Zhang. Ecvl-router: Scenario-aware routing for vision-language models. *arXiv preprint arXiv:2510.27256*, 2025.
- [32] Zihang Tian, Rui Li, Jingsen Zhang, Xiaohe Bo, Wei Huo, and Xu Chen. Haps: Hierarchical llm routing with joint architecture and parameter search. *arXiv preprint arXiv:2601.05903*, 2026.
- [33] Clovis Varangot-Reille, Christophe Bouvard, Antoine Gourru, Mathieu Ciancone, Marion Schaeffer, and Francois Jacquenet. Doing more with less – implementing routing strategies in large language model-based systems: An extended survey. *arXiv preprint arXiv:2502.00409*, 2025.

- [34] Ke Wang, Junting Pan, Weikang Shi, Zimu Lu, Mingjie Zhan, and Hongsheng Li. Measuring multimodal mathematical reasoning with math-vision dataset. *arXiv preprint arXiv:2402.14804*, 2024.
- [35] Peng Wang, Shuai Bai, Sinan Tan, Shijie Wang, Zhihao Fan, Jinze Bai, Keqin Chen, Xuejing Liu, Jialin Wang, Wenbin Ge, Yang Fan, Kai Dang, Mengfei Du, Xuancheng Ren, Rui Men, Dayiheng Liu, Chang Zhou, Jingren Zhou, and Junyang Lin. Qwen2-vl: Enhancing vision-language model’s perception of the world at any resolution. *arXiv preprint arXiv:2409.12191*, 2024.
- [36] Qixun Wang, Yang Shi, Yifei Wang, Yuanxing Zhang, Pengfei Wan, Kun Gai, Xianghua Ying, and Yisen Wang. Monet: Reasoning in latent visual space beyond images and language. In *Proceedings of the IEEE/CVF Conference on Computer Vision and Pattern Recognition*, 2026.
- [37] Wulin Xie, Yi-Fan Zhang, Chaoyou Fu, Yang Shi, Bingyan Nie, Hongkai Chen, Zhang Zhang, Liang Wang, and Tieniu Tan. Mme-unify: A comprehensive benchmark for unified multimodal understanding and generation models. *arXiv preprint arXiv:2504.03641*, 2025.
- [38] Rongchao Xu, Lin Jiang, Dahai Yu, Ximiao Li, and Guang Wang. Synhat: A two-stage coarse-to-fine diffusion framework for synthesizing human activity traces. *arXiv preprint arXiv:2604.14705*, 2026.
- [39] Yi Xu, Chengzu Li, Han Zhou, Xingchen Wan, Caiqi Zhang, Anna Korhonen, and Ivan Vulic. Visual planning: Let’s think only with images. *arXiv preprint arXiv:2505.11409*, 2025.
- [40] Jiaqi Xue, Qian Lou, Jiarong Xing, and Heng Huang. R2-router: A new paradigm for llm routing with reasoning. *arXiv preprint arXiv:2602.02823*, 2026.
- [41] Zhibo Yang, Jun Tang, Zhaohai Li, Pengfei Wang, Jianqiang Wan, Humen Zhong, Xuejing Liu, Mingkun Yang, Peng Wang, Lianwen Jin, and Junyang Lin. Cc-ocr: A comprehensive and challenging ocr benchmark for evaluating large multimodal models in literacy. *arXiv preprint arXiv:2412.02210*, 2024.
- [42] Shukang Yin, Chaoyou Fu, Sirui Zhao, Ke Li, Xing Sun, Tong Xu, and Enhong Chen. A survey on multimodal large language models. *arXiv preprint arXiv:2306.13549*, 2023.
- [43] Renrui Zhang, Dongzhi Jiang, Yichi Zhang, Haokun Lin, Ziyu Guo, Pengshuo Qiu, Aojun Zhou, Pan Lu, Kai-Wei Chang, Peng Gao, and Hongsheng Li. Mathverse: Does your multi-modal llm truly see the diagrams in visual math problems? *arXiv preprint arXiv:2403.14624*, 2024.
- [44] Tuo Zhang, Asal Mehradfar, Dimitrios Dimitriadis, and Salman Avestimehr. Leveraging uncertainty estimation for efficient llm routing. *arXiv preprint arXiv:2502.11021*, 2025.
- [45] Rui-Jie Zhu, Tianhao Peng, Tianhao Cheng, Xingwei Qu, Jinfa Huang, Dawei Zhu, Hao Wang, Kaiwen Xue, Xuanliang Zhang, Yong Shan, Tianle Cai, Taylor Kergan, Assel Kembay, Andrew Smith, Chenghua Lin, Binh Nguyen, Yuqi Pan, Yuhong Chou, Zefan Cai, Zhenhe Wu, Yongchi Zhao, Tianyu Liu, Jian Yang, Wangchunshu Zhou, Chujie Zheng, Chongxuan Li, Yuyin Zhou, Zhoujun Li, Zhaoxiang Zhang, Jiaheng Liu, Ge Zhang, Wenhao Huang, and Jason Eshraghian. A survey on latent reasoning. *arXiv preprint arXiv:2507.06203*, 2025.

Technical Appendices and Supplementary Material

A Additional Experimental Details

This appendix provides experimental details that are omitted from the main text for space. We first list the candidate MLLM pools used in each benchmark. We then describe how baselines are adapted to the benchmark setting, how model capability profiles are constructed, and how hyperparameters and random seeds are handled.

A.1 Candidate Model Pools

Both benchmarks define a fixed candidate model pool and provide per-model outcome annotations for each query. We follow the original benchmark model pools without adding or removing candidate models in the main experiments. MMR-Bench contains 11 candidate MLLMs, while VL-RouterBench contains 17 candidate MLLMs. Table 3 lists the full model pools used in our experiments.

Table 3: Candidate MLLM pools used in each benchmark.

Benchmark	# Models	Candidate MLLMs
MMR-Bench	11	Claude3-7V_Sonnet; GeminiFlash2-5; GeminiPro2-5; Gemma3-4B; InternVL3-78B; Qwen2.5-VL-3B-Instruct; Qwen2.5-VL-7B-Instruct; Qwen2.5-VL-72B-Instruct; gpt-5-2025-08-07; gpt-5-minimal-2025-08-07; gpt-5-nano-2025-08-07.
VL-RouterBench	17	deepseek_vl2; deepseek_vl2_tiny; GeminiFlash2-5; Gemma3-27B; GPT4o; InternVL2_5-78B; Janus-Pro-1B; Janus-Pro-7B; Kimi-VL-A3B-Thinking-2506; llama_next_vicuna_7b; MiMo-VL-7B-RL; Phi-3.5-Vision; Pixtral-12B; Qianfan-VL-8B; Qwen2.5-VL-32B-Instruct; Qwen2.5-VL-72B-Instruct; SmolVLM2.

A.2 Benchmark Metrics

We use the official metrics from each benchmark. For the performance-oriented setting, routers are evaluated by the answer quality of the selected model. For the performance-cost setting, routers are evaluated by the benchmark-native cost-aware metric. MMR-Bench reports normalized area under the cost-quality curve, denoted nAUC, which summarizes the quality-cost Pareto frontier across operating points. VL-RouterBench reports its official Rank Score, which measures routing quality under the benchmark’s prescribed cost-aware evaluation protocol. We do not introduce new evaluation metrics for the main comparison, so all reported numbers are comparable to the original benchmark protocols.

A.3 Baseline Adaptation

All trainable baselines are evaluated under the same data splits, candidate model pools, cost annotations, and router input features as LATENTROUTER. This ensures that differences in performance come from the routing method rather than from using different multimodal encoders, preprocessing pipelines, or training data.

For the feature-level baselines, KNNRouter, MLPMFRouter, and KMeansRouter use the benchmark-provided query features and follow the standard training and validation splits. These methods operate directly on feature-level representations and do not use the proposed routing capsules, model capability tokens, latent communication layers, or distributional outcome head.

For learned router baselines, we adapt ECVL [31], RouteLLM [27], and RouterDC [5] to the same MLLM routing setting. ECVL is included as a recent vision-language router baseline. RouteLLM and RouterDC are originally designed for text-based LLM routing, so we provide them with the same benchmark-provided multimodal query features and candidate-pool information used by other trainable routers. When a baseline requires pairwise preferences or model labels, we derive them from the per-model outcome annotations on the training split. Hyperparameters for all baselines are selected on the validation split and fixed before test evaluation.

A.4 Model Capability Profiles

LATENTROUTER represents each candidate MLLM with a model capability token. The input to this token includes model-level calibration statistics, normalized cost, latency, and available slice-level or pairwise behavior. These statistics are computed only from the training or calibration split, never from the test split.

The calibration profile summarizes how well each model performs overall and, when the benchmark provides task or scenario annotations, how well it performs on different slices such as OCR, document understanding, chart reasoning, STEM reasoning, or general VQA. Pairwise behavior summarizes how often a model outperforms other candidate models on calibration examples. These statistics are normalized before being projected into the hidden space used by LATENTROUTER. This profile construction allows the router to compare candidate models through model-level capability representations rather than relying on a fixed classifier over model IDs.

A.5 Training, Validation, and Seeds

All trainable methods are trained on the official training split, tuned on the validation split, and evaluated on the test split. Hyperparameters are selected using validation performance under the corresponding routing setting and are then fixed for final test evaluation. Unless otherwise specified, we report results over three random seeds. The reported error bars are computed across these seeds.

For LATENTROUTER, the main hyperparameters include the number of routing capsules C , the number of latent communication layers H , the hidden dimension, the residual bound ρ , the cost tradeoff parameter λ , and the loss weights for the distributional, pairwise, listwise, utility, and residual regularization terms. The main experiments use $C = 7$ routing capsules and $H = 2$ latent communication layers unless otherwise stated.

A.6 Additional Implementation Details

All routers use the same benchmark-provided preprocessed files, including image features, question features, side features, model-pool metadata, cost annotations, and model-outcome traces. Unavailable models are masked during attention and scoring. Costs are normalized within each benchmark before being used in cost-aware routing. Model capability profiles are recomputed separately for each benchmark to avoid mixing statistics across different candidate pools or evaluation protocols.

For LATENTROUTER, the distributional outcome head predicts a mean and uncertainty for each candidate model. The bounded capsule correction is applied to the predicted mean before computing the final utility score. The same outcome head is shared across candidate model tokens, which allows the router to score the available model pool without changing the output dimension.

B Theoretical Analysis

This section provides formal details for the theoretical claims used in the main text. Section B.1 formalizes why MLLM routing requires query-model interaction. Section B.2 proves that the bounded capsule correction cannot overturn sufficiently confident base rankings. Section B.3 shows why shared per-model scoring with availability masking is compatible with changing candidate pools.

B.1 Need for Query-Model Interaction

The main text argues that MLLM routing should model interactions between query requirements and model capabilities. The following proposition makes this precise.

Proposition B.1 (Need for query-model interaction). *Suppose there exist two queries x, x' and two models m_i, m_j such that*

$$y_i(x) > y_j(x), \quad y_i(x') < y_j(x').$$

Then no additive scoring rule of the form

$$s(x, m) = g(x) + h(m)$$

can correctly rank m_i and m_j for both queries.

Proof. For an additive score,

$$s(x, m_i) - s(x, m_j) = (g(x) + h(m_i)) - (g(x) + h(m_j)) = h(m_i) - h(m_j).$$

The query-dependent term $g(x)$ cancels out. Therefore, the sign of the pairwise margin between m_i and m_j is independent of the query x . The additive router must always rank m_i above m_j , or always rank m_j above m_i , for every input.

However, by assumption, the correct ranking reverses across two queries:

$$y_i(x) > y_j(x), \quad y_i(x') < y_j(x').$$

Thus, an additive scoring rule cannot correctly represent both rankings. A router must include a query-model interaction term, such as

$$s_\theta(x, m_i, \mathcal{M}) = f_\theta(R(x), a_i, A),$$

where $R(x)$ represents query-dependent multimodal routing signals and a_i represents the capability token of model m_i . \square

Note that this proposition does not claim that LATENTROUTER is the only possible interaction architecture. It only rules out purely additive scoring functions whose pairwise model ordering is independent of the query.

B.2 Stability of the Bounded Capsule Correction

The main text uses a bounded capsule correction to refine close predictions without letting residual signals dominate the base outcome estimate. The following proposition formalizes this stability:

Proposition B.2 (Bounded residual stability). *Let*

$$\tilde{\mu}_i = \mu_i + \Delta_i^{\text{cap}},$$

where

$$|\Delta_i^{\text{cap}}| \leq \rho$$

for all candidate models m_i . For any two models m_i, m_j , if

$$|\mu_i - \mu_j| > 2\rho,$$

then the bounded capsule correction cannot reverse their ranking.

Proof. The corrected pairwise margin is

$$\tilde{\mu}_i - \tilde{\mu}_j = (\mu_i + \Delta_i^{\text{cap}}) - (\mu_j + \Delta_j^{\text{cap}}) = (\mu_i - \mu_j) + (\Delta_i^{\text{cap}} - \Delta_j^{\text{cap}}).$$

Because each correction is bounded by ρ ,

$$|\Delta_i^{\text{cap}}| \leq \rho, \quad |\Delta_j^{\text{cap}}| \leq \rho.$$

By the triangle inequality,

$$|\Delta_i^{\text{cap}} - \Delta_j^{\text{cap}}| \leq |\Delta_i^{\text{cap}}| + |\Delta_j^{\text{cap}}| \leq 2\rho.$$

Therefore, the correction can change the base margin by at most 2ρ in magnitude. If

$$|\mu_i - \mu_j| > 2\rho,$$

then the correction cannot change the sign of the pairwise margin. Hence, the corrected scores $\tilde{\mu}_i$ and $\tilde{\mu}_j$ preserve the same ranking as the base scores μ_i and μ_j . \square

Scope. This result does not guarantee that the bounded correction always improves routing accuracy. It only shows that the correction acts as a controlled adjustment: it can affect uncertain or close decisions, but it cannot overturn rankings whose base margin is larger than 2ρ .

B.3 Shared Scoring under Changing Model Pools

LATENTROUTER scores candidate models through shared model capability tokens and masks unavailable models. This design supports changing candidate pools without requiring a fixed classifier over model IDs. We formalize this property as permutation equivariance over available model tokens.

Proposition B.3 (Permutation equivariance of shared per-model scoring). *Let $A = \{a_1, \dots, a_K\}$ be the set of model capability tokens and let $\Omega(x)$ be the availability mask. Suppose the latent communication layers use shared attention parameters, shared feed-forward parameters, and availability-masked self-attention over model tokens. Suppose the outcome head g_θ is shared across model tokens. For any permutation π of the model-token order, if both the model tokens and availability mask are permuted consistently, then the predicted scores are permuted in the same way:*

$$s_\theta(x, m_{\pi(i)}, \pi(A), \pi(\Omega)) = \pi(s_\theta(x, m_i, A, \Omega))_i.$$

Proof. Cross-attention from model tokens to routing capsules applies the same attention parameters to each model token. Therefore, permuting the order of model tokens permutes the corresponding cross-attended model states in the same way. Availability-masked self-attention over model tokens is also permutation equivariant when the availability mask is permuted consistently, because attention weights depend on token content and mask entries, not on absolute model positions. The feedback attention from routing capsules to model tokens aggregates over the same permuted set of available model states, so the capsule update is invariant to model-token order up to the corresponding permutation of model states. Finally, the shared outcome head g_θ is applied independently to each final model token. Therefore, permuting model tokens and their availability mask produces the same permutation of predicted scores. \square

This property explains why LATENTROUTER can score different available model subsets through masking and shared per-model scoring. It does not by itself guarantee good performance on newly added models; reliable new-model routing still depends on informative model capability profiles.

C Additional Experiments

This appendix provides additional experimental details and supporting results omitted from the main text for space. We include task-group construction, full ablation values, model-pool flexibility statistics, efficiency numbers, and additional sensitivity and cold-start analyses.

C.1 Task Group Construction

For task-level analysis, we group datasets from MMR-Bench and VL-RouterBench into coarse categories according to the benchmark-provided task or scenario definitions. The radar plot in Figure 2c uses these groups only for analysis; all routers are trained and evaluated on the official benchmark splits.

Table 4: Mapping from benchmark datasets to coarse task groups.

Task Group	MMR-Bench Datasets	VL-RouterBench Datasets
OCR / Document QA	OCRBench, SEED-Bench v2 Plus	DocVQA, TextVQA, OCRBench
Chart / Diagram	–	ChartQA, AI2D
Math / STEM	MathVista, MathVision, MathVerse	MathVista, MathVision, MathVerse
General VQA / Grounding	MMStar, RealWorldQA	MMBench, MMStar, MMMU, RealWorldQA, InfoVQA, HallusionBench

C.2 Full Ablation Results

Table 5 gives the full ablation numbers corresponding to Figure 3b. The full model is strongest across all four settings. Removing latent communication gives the largest average degradation, while removing model capability tokens or routing capsules also consistently hurts. These results support the interpretation that LATENTROUTER benefits from both sides of the latent capability-matching design: query-side routing capsules and model-side capability tokens.

Table 5: Full ablation results. Columns follow the same order as Table 1.

Variant	MMR-Oriented	MMR-Cost	VL-Oriented	VL-Cost
Full LATENTROUTER	0.792±0.001	0.786±0.001	0.815±0.001	0.812±0.003
w/o routing capsules	0.770±0.002	0.768±0.002	0.797±0.003	0.799±0.002
w/o model capability tokens	0.766±0.003	0.764±0.002	0.789±0.004	0.791±0.003
w/o latent communication	0.758±0.002	0.756±0.002	0.781±0.004	0.783±0.003
w/o distributional prediction	0.764±0.002	0.762±0.002	0.792±0.003	0.794±0.002
w/o bounded correction	0.776±0.002	0.774±0.001	0.784±0.002	0.784±0.001

C.3 Model-Pool Flexibility Details

Table 6 reports the full mean \pm standard deviation values for model-pool flexibility. For each modified pool, oracle and fixed-model baselines are recomputed over the available models only. The one-available-model setting has zero oracle regret because the available model is also the pool oracle.

Table 6: Model-pool flexibility under changed candidate pools. Primary Metric averages the four main benchmark settings.

Pool Setting	Primary Metric \uparrow	Oracle Regret \downarrow	Latency (ms) \downarrow
Full pool	0.801±0.002	0.128±0.018	0.052±0.004
Remove strongest	0.756±0.018	0.151±0.021	0.050±0.004
Remove cheapest	0.792±0.013	0.130±0.017	0.051±0.004
Remove random 30%	0.779±0.017	0.139±0.020	0.047±0.003
Leave-one-model-out	0.784±0.015	0.135±0.019	0.050±0.004
One available model	0.731±0.041	0.000±0.000	0.018±0.002

C.4 Efficiency Details

Table 7 provides the numerical efficiency values used in Figure 4. Avg. Primary is computed from the same four main settings in Table 1: MMR-oriented, MMR-cost, VL-oriented, and VL-cost. Router latency measures only the router forward pass and excludes selected MLLM inference time.

Table 7: Router-side efficiency. Avg. Primary is averaged over the four main benchmark settings in Table 1.

Method	Avg. Primary \uparrow	Router Latency (ms) \downarrow	Router Size (M) \downarrow
KMeansRouter	0.770 \pm 0.002	0.11 \pm 0.01	1.4
ECVL	0.759 \pm 0.000	0.13 \pm 0.01	1.8
RouteLLM	0.715 \pm 0.004	0.17 \pm 0.02	2.4
RouterDC	0.654 \pm 0.005	0.10 \pm 0.01	1.2
GraphRouter	0.751 \pm 0.006	0.14 \pm 0.02	1.9
R2-Router	0.759 \pm 0.006	0.16 \pm 0.02	2.1
LATENTROUTER	0.801 \pm 0.002	0.06 \pm 0.01	0.9

The efficiency comparison supports a practical interpretation of the method. LATENTROUTER obtains the strongest average primary metric while using the smallest and fastest router among learned methods. The comparison with GraphRouter and R2-Router is especially informative: interaction-based routers can improve over simple feature-level routing, but LATENTROUTER achieves a better quality–efficiency tradeoff by using lightweight shared model-token scoring and a compact capsule-token communication module. This suggests that the gains are not explained by a larger router, but by the routing-specific inductive bias for matching multimodal query requirements with candidate model capabilities.

C.5 Cold-Start Model Insertion

To further test model-pool flexibility, we evaluate whether LATENTROUTER can score a newly inserted or held-out model. For each benchmark, we hold out one candidate model during router

training, compute its capability profile from a small calibration subset, and insert it back into the candidate pool at test time. The router must score the held-out model through its capability token rather than through a learned fixed model-ID classifier.

Table 8: Cold-start model insertion with different calibration sizes. Results report the average primary metric across benchmarks.

Calibration examples per held-out model	Avg. Primary \uparrow	Oracle Regret \downarrow
0	0.771 \pm 0.006	0.153 \pm 0.008
16	0.781 \pm 0.005	0.142 \pm 0.007
64	0.789 \pm 0.004	0.134 \pm 0.006
128	0.793 \pm 0.003	0.130 \pm 0.005
Full calibration	0.801 \pm 0.002	0.128 \pm 0.004

Performance improves smoothly as more calibration examples become available. With no calibration examples, the router is still usable but less accurate because the new model token lacks reliable capability statistics. With 64–128 examples, performance approaches the full-calibration setting. This supports the model-token design: new candidate MLLMs can be inserted without changing the router architecture, but reliable routing still benefits from representative calibration data.

C.6 Sensitivity to Routing Capsules

We also vary the number of routing capsules C . Table 9 shows that performance improves from $C = 1$ to $C = 7$, indicating that multiple capsules help preserve different multimodal routing signals. Increasing to $C = 12$ does not yield further improvement, so we use $C = 7$ as the default configuration.

C.7 Live Model API Validation

We further validate whether LATENTROUTER can execute the deployment path with actual model calls. The live pool contains five locally served vision-language models through Ollama: llama3.2-vision, gemma3, llama:7b, moondream, and minicpm-v. We evaluate on a held-out VL-RouterBench subset covering Chart/Diagram, General VQA, Math/STEM, and OCR/Document QA. For each query, every deployable router selects exactly one model before observing any answer. All models pass the availability check, and all calls succeed. Since the models are locally served, configured monetary cost is zero; we therefore report quality, latency, and a quality-latency score.

Table 10 shows that LATENTROUTER achieves the best live quality and the best quality-latency score while maintaining moderate latency. Unlike fixed policies, it selects different models for different queries, confirming that the learned policy performs query-dependent model selection in the live pool. On a diagnostic oracle subset, the oracle upper bound reaches quality 0.542, while LATENTROUTER obtains the smallest deployable oracle regret. This live validation is complementary to the offline benchmarks: the offline results provide controlled routing evidence, while the live study verifies that the same routing pipeline works under real model-call conditions.

D LLM Usage

Large language models were used only for writing assistance, including grammar checking, wording refinement, formatting suggestions, and readability editing. They were not used to generate the core methodology, design experiments, produce experimental results, create evaluation labels, or make routing decisions. All technical claims, mathematical formulations, experimental settings, and reported results were checked and finalized by the authors.

E Limitation

This work has a few limitations that suggest natural directions for future study. First, our experiments follow the offline evaluation protocols of MMR-Bench and VL-RouterBench, where per-model outcome annotations are available for controlled router comparison. This is the standard setting for

Table 9: Sensitivity to the number of multimodal routing capsules C .

Setting	Avg. Primary \uparrow	Avg. Oracle Regret \downarrow
$C = 1$	0.781 \pm 0.004	0.143 \pm 0.006
$C = 4$	0.790 \pm 0.003	0.135 \pm 0.005
$C = 7$	0.801\pm0.002	0.128\pm0.004
$C = 12$	0.795 \pm 0.003	0.129 \pm 0.005

Table 10: Live model API validation. Quality is the benchmark-compatible answer score (\uparrow), latency is selected-model wall-clock latency in seconds (\downarrow), and Q-L score is Quality $- 0.05 \cdot$ Latency (\uparrow).

Router	Quality \uparrow	Latency \downarrow	Q-L Score \uparrow
LATENTROUTER	0.458	0.610	0.428
Strongest	0.375	0.530	0.349
Random	0.333	0.780	0.294
Cheapest	0.292	0.490	0.268

current routing benchmarks, but live deployment may involve additional factors such as changing model versions, API availability, dynamic pricing, and latency variation. Second, LATENTROUTER uses calibration statistics to construct model capability tokens. The framework can support changing model pools through these tokens, but newly added models still benefit from representative calibration examples. Third, our evaluation focuses on benchmark-defined image-question routing tasks. Extending the same formulation to open-ended multimodal agents, multi-step tool use, or interactive routing remains an interesting direction. Finally, the routing capsules are learned latent states rather than human-readable explanations. They improve model selection, but they should not be interpreted as faithful natural-language rationales. Future work can study stronger interpretability tools, live-system evaluation, and more adaptive calibration for evolving MLLM pools.

F Broader Impact

MLLM routing can have positive practical impact by making multimodal AI systems more efficient and accessible. Instead of always calling the largest or most expensive MLLM, a router can select a model that is sufficient for the current query, potentially reducing inference cost, latency, and energy consumption. This can make multimodal systems easier to deploy in resource-constrained settings and can support more flexible use of heterogeneous open-source and closed-source model pools. At the same time, routing introduces additional risks. A cost-aware router may sometimes select a cheaper but less capable model, which could reduce answer quality on difficult or safety-sensitive queries. This is especially important in domains where multimodal errors may have high consequences, such as medical, legal, financial, accessibility, or public-sector applications. A deployed router should therefore include appropriate safeguards, such as confidence thresholds, fallback to stronger models, monitoring of failure cases, and task-specific restrictions for high-risk settings. Routing can also affect fairness and reliability. If calibration data underrepresents certain languages, visual styles, document formats, cultural contexts, or accessibility-related inputs, the router may learn inaccurate capability profiles and route those queries to weaker models. Periodic recalibration and evaluation across diverse user groups and input types are therefore important. In addition, because LATENTROUTER uses benchmark-provided model outcomes and model-level metadata, any biases or errors in the underlying candidate MLLMs can be inherited by the routing policy. The router should be viewed as a model-selection mechanism, not as a guarantee of correctness or safety. Finally, model-pool routing may increase dependence on proprietary model APIs if the best-performing or best-calibrated models are closed-source. We encourage transparent reporting of model versions, costs, latency assumptions, and calibration protocols when deploying or evaluating routing systems.